Response to Reviewers: Urban ozone formation and sensitivities to volatile chemical products, cooking emissions, and NO_x across the Los Angeles Basin

We appreciate all the reviewers' comments and suggestions. We have made every effort to incorporate these suggestions to improve the manuscript. Below, we address the referee comments (in black), and provide our responses (in blue).

Referee #1

Stockwell et al. 2024 take advantage of a Lagrangian model armed with state-of-the-art VOC and NOx emissions and chemistry over a region undergoing degraded air quality to study the sensitivity of surface ozone to various emissions. The authors found some exciting new contributors to augmenting ozone in LA, such as the contribution of cooking emissions and personal products. Attributing what emission types control PO_3 and where the non-linearities of PO_3 are located is essential to better implementing emission mitigation. This type of work is usually practiced with CTM models because it can provide much larger data points and a more suitable treatment of non-local and local vertical mixing. However, having a more straightforward but effective tool is appreciated. The paper has some important new messages for controlling ozone pollution in the region; nonetheless, there are many ambitious points about the modeling framework, and the paper should extend the number of receptor points to capture better the complete picture of ozone sensitivity in the region. If an algorithm proves to be faster, it is likely to be reflected in more runs, necessitating the addition of more receptors. I recommend the publication of this work after major revisions.

We thank the Referee for their extensive and thorough comments and we have updated the text to clarify the benefits and limitations of a box model compared to a CTM, as each has its own strengths. Here, the Lagrangian box model is meant as a tool that complements understanding of the processes that are difficult to represent in 3D models. We have used similar approaches previously (e.g. Coggon et al. 2021) to investigate ozone responses to detailed changes to emissions and chemical mechanisms for WRF-Chem simulations used in New York City (NYC). Similarly, this box model is complementary to the WRF-Chem simulation described by Zhu et al. (2024a) and updated in the recently submitted Zhu et al. (2024b, submitted).

We appreciate the reviewer's comment to extend the number of receptor points, however, this is beyond the scope of this work. The model is intended to understand the atmospheric chemistry of air upwind and at the location of the Pasadena and Redlands receptor sites. The box model does not cover the spatial domain of a 3D model, and its advantage over a purely Eulerian box model is that it informs non-linearities in ozone production along its trajectory path, as well as at the Pasadena super-site. The spatial statistics are necessarily limited in our approach, since trajectory paths are not identical each day due to varied meteorology. To illustrate this distinction between a trajectory box model, an Eulerian box model, and a CTM, we add language to the text to emphasize

this point as outlined in our responses below. We also updated the manuscript title and language throughout the text to narrow the scope to focus on the model simulation and ozone formation and response upwind and at the receptor sites instead of generalizing conclusions to the entire Los Angeles Basin.

Major comments

Poor description of the modeling framework: *The description of the modeling framework is unclear and contains ambiguous points. The model calculates backward trajectories based on WRF-FLEXPART arriving at two separate stations in LA's downwind. For each 15-minute interval trajectory, Eq.1 is used to dilute any primary emissions over a box of 8 km x 8 km x PBLH, resolve chemical source/sinks by F0AM, and consider dilution/entrainment based on PBLH and some prescribed background concentrations. This model is a simplified version of a CTM model in a Lagrangian framework, ignoring cloud chemistry, vertical diffusion, convective transport, and dry deposition. The description of the modeling part needs serious refinement. For instance, the photolysis rates are mentioned in different subsections with a questionable correction factor stating that "the WRF-Chem calculated photolysis frequencies were scaled using observed NO2 photolysis rates at the ground site (jNO2) ratioed to WRF-modeled jNO2". How can a single measurement at a given location constrain photolysis rates in all backward trajectories going over different surface albedo, aerosol/cloud cover, and solar irradiance at different times? The same applies to meteorology. The authors stated: "The model was constrained with meteorological measurements of pressure, temperature, and relative humidity conducted at the ground site." How were meteorological measurements treated for all trajectories? Where are the Doppler LiDAR measurements, and how were they used to correct PBLH over this many trajectories? Are all these trajectories passing through the PBL region (because that's how the authors have diluted the emissions)? How does the F0AM model work in this algorithm? Does the model cycle with the sun so that it can approach a steady state? Are we assuming a steady state for chemistry? Dry deposition is a large sink for surface ozone; where is its exclusion being compensated for? I highly recommend adding a flowchart explaining how each component is adjusted or constrained and its connections to the other elements.*

Our model is completely dependent on processes outlined in Eq. (1). Originally, Section 2.2 provided a general overview of the model framework, while Sections 2.2.1 – 2.2.4 addressed how we implement each of the terms in Eqn. (1), including the emissions, chemical reactions, and dilution processes. As recommended by both referees, we have reorganized Sect. 2.2 to include a brief description of the previously published complementary CTM analysis (Zhu et al., 2024a), followed by subsections that include a generic box model description followed by the original, yet modified, subsections that describe each term in Eq. (1). Other important clarification points were necessary and the following discussion describes additional modifications to the text based on the above comments/questions.

Description and framework: We have reorganized the overview text at the beginning of Sect. 2.2 to eliminate redundancies and to create better flow and include a general box model description as its own subsection. Additionally, we added a visual representation of Lagrangian box models in Supplemental Fig. S1.

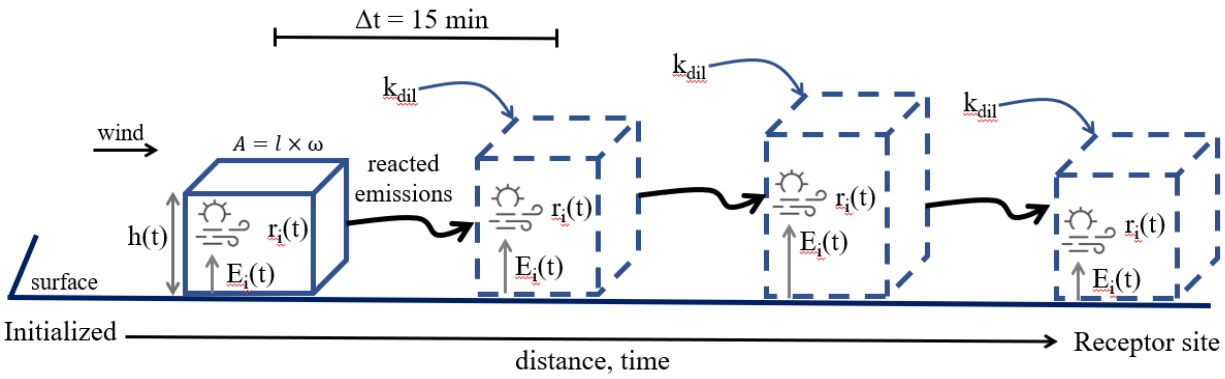

Figure S1: *A simplified representation of the Lagrangian trajectory box model, shows a well-mixed volume of air extending from the surface to the height of the boundary layer (h) within a defined area footprint (A). Each box model step is a coordinate (latitude, longitude, time) determined every 15-minutes along a trajectory path moving with the wind towards a receptor site. The starting mixing ratios in the initial box (solid box) or resulting from a previous model step (dashed box) are combined with a corresponding emission flux (E_i) from the surface. The contents are assumed to mix and chemically process (r_i) over the model step interval (Δt =15 min). The mass exchange with the air above and to the sides is represented by entrainment with background air (k_{dil}), which is estimated from changing boundary layer heights between model steps.*

Photolysis frequencies, Photolysis frequencies (J-values) were retrieved from WRF-Chem simulations using the TUV model linked to the RACM2B-VCP mechanism scheme as described by Zhu et al. (2024a) and in Sect. 2.2.4 (now 2.2.5). The J-values do vary along the trajectory path based on time, location, meteorology, surface albedo etc.; however, we compare the measured jNO_2 to WRF-modeled jNO_2 at the endpoint (in Pasadena). From the jNO_2 bias determined at the endpoint, we assume the same upwind bias along the trajectory path. Similar corrections using observations are suggested by Wolfe et al. (2016). This means that local effects, such as cloud coverage, are captured by the WRF-model along the trajectory, while the broad-scale effects, such as solar zenith angle or high-altitude aerosol scattering are corrected for biases observed at the Pasadena site. Bias-correcting the J-values using endpoint observations generally lowered WRF-derived photolysis frequencies during the day by 15-20%. We have modified the text as follows:

"Photolysis frequencies account for photon attenuation by clouds or highly absorbing aerosol (e.g., biomass burning smoke) and varied in space and time. The WRF-Chem calculated photolysis frequencies along each Pasadena trajectory were bias-corrected using observed NO_2 photolysis rates (jNO_2) comparisons with WRF-modeled jNO_2 at the receptor site. This assumption generally lowered upwind daytime photolysis frequencies by 15-20%. Measured jNO_2 was interpolated during periods when shadows blocked instrument retrievals"

Meteorology & PBLH: From the Referee's comments and suggestions, we have updated the box model to use WRF-Chem PBLH and meteorology (T,P,RH) along the transport pathways and only constrained to local PBLH observations at the receptor site in Pasadena. This should better represent varying meteorology and boundary layer heights spatially and not just temporally. The model now accounts for time- and space-varying meteorology, photolysis frequencies, and dilution instead of constraining completely using receptor site measurements. With the updates to the meteorology and PBLH within the box model, we have updated every figure in the manuscript.

Finally, we have also added the following text to Sect. 2.1 to emphasize PBLH measurements were conducted in Pasadena and used to constrain only at the Pasadena endpoint:

"The Stationary Doppler lidar On a Trailer (StaDOT) was co-located at the Pasadena site and measured the planetary boundary layer height."

Box model steady-state & deposition: We are accounting for time- and location-varying emission sources along each trajectory path and the aim is not to reach a steady-state condition, but rather to accurately represent conditions and reproduce observed variability at a ground site across a month-long sampling period. This model considers trajectory path, emissions, meteorology, and accounts for the upwind history of the air mass for several hours before arriving in Pasadena or Redlands, and is not a steady-state model.

As discussed in the text most deposition is ignored and dilution is the only physical loss. Experimental deposition velocities are limited and parameterizations are complicated by meteorology, surface variability, and chemical interactions. If we assume a daytime deposition velocity (0.1 cm s^{-1}; Clifton et al. (2020)), PBLH (1000 m), and transport time (4.5 h^{-1}), we'd expect a 1.6% loss of the total ozone across the trajectory path.

Excessive dilution within the PBL: *From my understanding, any VOC or NOx emissions within the PBL (it could be mobile sources at the surface layer or a large chimney at higher altitudes) are diluted uniformly within the PBL (the first term in Eq1). This means that the authors are overly simplifying non-local and local vertical diffusion components typically parameterized in Eulerian models such as WRF-Chem. This will lead to some underestimation/overestimation issues, especially for short-lived species, including NOx and isoprene. The vertical distribution of these species rapidly declines within the PBL. Even under an expanded PBL height and considerable turbulence, it is unlikely for some of these critical compounds to be fully well-mixed. A vertically-mixed situation is only applicable to long-lived species such as ozone and CO. So, the current framework must have representative issues concerning photochemical ozone conditions because, realistically, there is a vertical dependency of PO_3 sensitivity to NOx and VOC within the PBL height that is overlooked here. This representativity issue needs to be studied and carefully conveyed as a limitation in the conclusion.*

There are inherent limitations when running simple models (Jacob, 1999), with a primary simplification being that emissions are assumed to be well-mixed within a defined box volume. The model step time resolution is 15 minutes to allow for mixing within the height of the boundary layer. If we assume a convective velocity scale on the order of 1.38 m/s (determined from the measured lidar daytime vertical velocity variance), the time-scale of mixing through a daytime PBLH (approx. 700-1000 m) would be 9-12 minutes. It can therefore be assumed that emissions are well-mixed within each 15-minute timestep, though, this gives no information on the vertical gradient of short-lived species.

There can also be underestimation/overestimation depending on the assumed dilution. This model constrains dilution using entrainment rates estimated from time-varying PBL heights. The comparisons for most species with surface measurements show good agreement, even for shorter-lived compounds such as NO_x as discussed in Sect. 3. While changing the dilution will impact the

absolute mixing ratios for all species, we have run two additional sensitivity tests to show that changes to the dilution factor have negligible impacts on the conclusions of our O_3 sensitivity tests to NO_x changes.

The figure below shows the O_3 sensitivity to NO_x at 2 PM in Pasadena for our original base simulation (red), and when dilution is increased (yellow) and decreased (blue) by 25%. The vertical dotted line is the initial NO_x emissions and the vertical hashes represent the point where O_3 transitions from NO_x saturated to NO_x sensitive ozone production. This is similar to the original Fig.6 in the main manuscript. While the absolute values of O_3 mixing ratios change with dilution, each simulation shows that Pasadena is near the transition point and approximately a 10% reduction in NO_x would result in this transition. Similarly, while the absolute contributions of individual AVOC sectors to O_3 might differ with dilution, the relative contributions would remain the same.

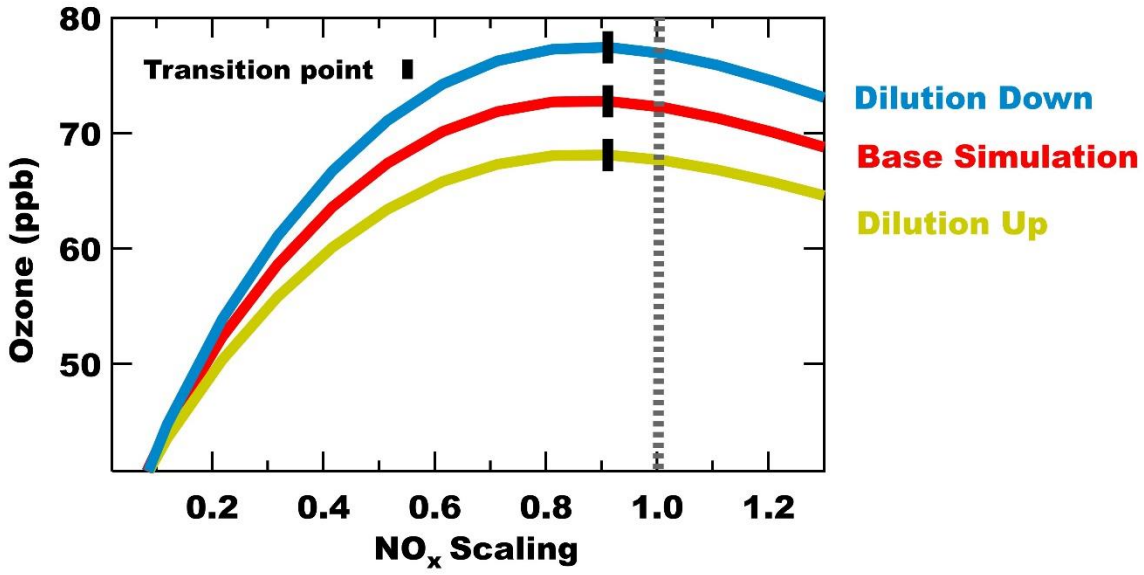

A forthcoming paper includes a complementary analysis using WRF-Chem across the LA Basin (Zhu et al., 2024b), and shows Pasadena is also near the transitional regime. Thus, the simplified well-mixed boundary layer assumptions in the box model reach a similar conclusion as CTMs that implement a more complex vertical mixing and diffusion scheme.

In response to a comment by Referee #2, we also update Figure 6 to show the campaign average MDA8 O_3 instead of averaged O_3 at 14:00 LT. We also repeated this analysis for the mean MDA8 instantaneous net ozone production rate (PO_3, ppb h^{-1}) to show similar responses in a new supplemental figure (Fig. S13). Please see the detailed justification in response to Referee #2.

Investigating the vertical dependency of O_3 sensitivity to NO_x and VOC is not possible with a box model that assumes mixing through the height of the boundary layer. We have added the following text to the manuscript to clarify this:

"The O_3 responses to NO_x perturbations are estimated for all of the modeled trajectories within a well-mixed boundary layer and therefore does not represent effects due to gradients in shorter lived species"

Representativeness of the whole LA Basin: *This study focused on two receptor sites to generalize the sensitivity of PO_3 to different VOC types and NOx emissions. While one of these sites is a supersite measuring a vast number of geophysical variables, they are influenced by a limited number of atmospheric conditions (both chemistry and meteorology) along with the trajectories that may only be representative of some physiochemical processes transpiring in the LA basin. In other words, a limited number of trajectories (which move by time and space and do not sample uniformly like how an Eulerian model does) limits the degree of generalizability of the conclusions made from this work. If, hypothetically, we had 100 supersites uniformly spreading over the domain, would the conclusion change? Some of the statistics related to the supersite are also not indicative of how the model performs over the LA. For instance, it is challenging to attribute the isoprene biases over the Pasadena site to the isoprene emission over the whole region. The last air parcel over the supersite doesn't fully remember all the physicochemical processes happening back in the trajectory. The authors included another site with limited observations to expand their analysis, but this has raised a legitimate question: if this modeling framework is much more efficient than WRF-Chem, what is preventing the authors from applying the same algorithm on many EPA's surface sites to boost the confidence in the results and attribution of LA ozone to LA's emissions.*

The Lagrangian box model is ideal for interpretation of the detailed simulation arriving at a well-equipped supersite, in this case Pasadena. The trajectory-based model expands to provide insight into the upwind meteorology, emissions, chemistry, and processing and accounts for physicochemical processes. We do recognize we are limited spatially to areas where the trajectories frequently pass and therefore we expand the discussion on this limitation and update Figures as detailed below. Additionally, we restrict the scope of the manuscript by changing the title and language to focus on ozone formation and response in and upwind of those receptor sites and no longer generalize the discussion to the Los Angeles Basin.

At each receptor site we have good temporal statistics since the trajectory endpoint arrives at that specific location every hour spanning a month. However, we agree that we do not get the same level of statistics in other areas along the trajectory paths since the track is not identical day to day as it varies with meteorology. Figure 5A was intended to spatially grid $\Delta NO_x|_{transition}$ so that the parcel tracks shown in Supp. Fig. S8 (now S13) were not stacked and disguising the predominate color scheme for all trajectories. However, once gridded there were occasionally not many data points included in the average. Instead we have now gridded the trajectories onto a coarser resolution (8 × 8 km) to match the resolution of the box model. The grids are now the average, considering only times and locations between 12:00-20:00 LT, where the total number of data points exceeded 50. This eliminates grids where the average was restricted to only a few data points and the updated Fig. 5A is shown below. We also ran additional tests, where we estimated the average trajectory path in that timeframe to Pasadena and Redlands, each. Along the average track from the coast, we then bounded the path within +/-8 km for ~4 km length segments. The average $\Delta NO_x|_{transition}$ for each bin is colored below, where the number of data points (n) ranged between 79-644. This figure has been added to the supplement. We also show $\Delta NO_x|_{transition}$ as a

function of distance from the coastline, also colored by $\Delta NO_x|_{transition}$ that will now be included in Figure 5B. This approach shows a similar representation of the changing ozone sensitivities to NO_x spatially along the trajectory paths with improved statistics. The updated Figure 5 and new Figure S14 are shown with their updated captions below.

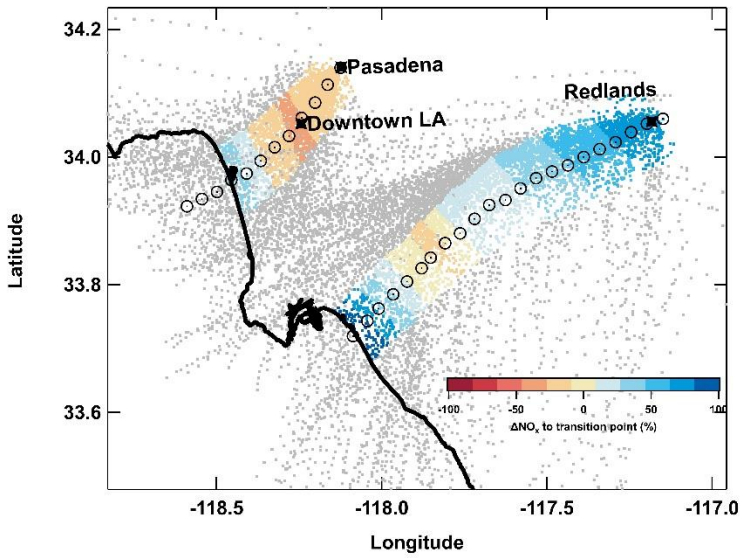

Figure S14: The trajectory paths to Pasadena and Redlands, CA averaged from 12:00-20:00 LT (black markers) and overlaid with all backward trajectory parcel tracks (grey dots). The average change in NOx emissions required to reach the transition within ± 8 km of each average trajectory path in 4 km segments is shown where warmer colors (-%) indicate the location is currently NOx–saturated, while cooler (+%) is NOx–limited.

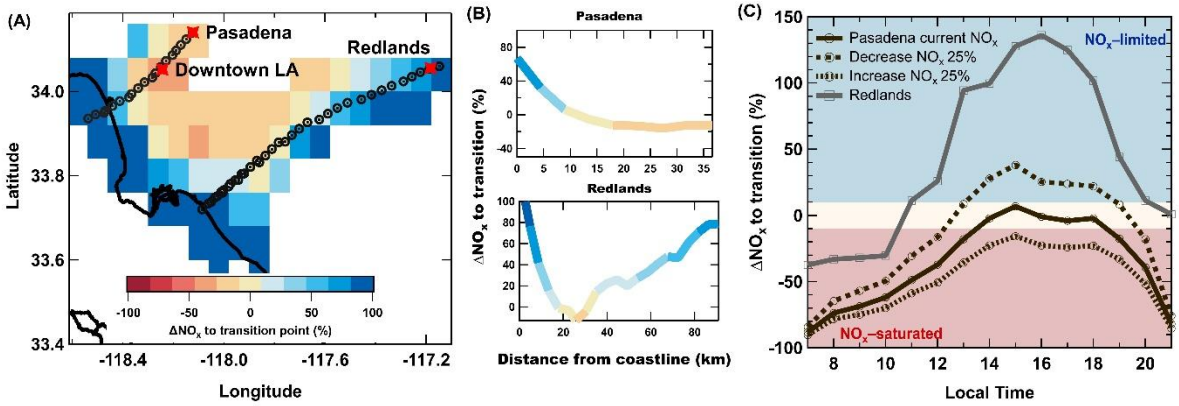

Figure 5: (A) The NOx emissions required to reach the transition between chemical regimes (□NOx|transition, %) averaged in 8 × 8 km grids for times between 12:00-20:00 LT, only where n>50. Warmer colors (–%) indicate the location is currently NOx–saturated, cooler (+%) is NOx–limited, and neutral (pale yellow) indicates nearing a transitional regime (□NOx|transition = +/- 10%). The average trajectory path to Pasadena and Redlands is

indicated by black markers. (B) The average NOx emissions required to reach the transition within +/- 8 km of each average trajectory path is shown in Fig. 5B as a function of distance from the coastline (km) to Pasadena (top middle) and Redlands (bottom middle). (C) The predicted average (solid line) change in NOx needed to transition between photochemical O3 chemical regimes for the month of August, 2021 in Pasadena, CA. Red shading designates the current chemical regime as NOx–saturated, blue shading designates NOx–limited. The dashed lines simulate the sensitivity as the base case NOx is increased and reduced by 25%. The solid grey line designates sensitivity results in Redlands, CA.

Minor comments:

I highly recommend replacing the NOx-saturated regime with the VOC-sensitive term throughout the paper. This is primarily because "NOx-saturated" tends to overemphasize the positive effect of NOx reduction on PO3 instead of the negative effect of VOC reduction. As a matter of fact, even in NOx-saturated regimes, it is important to reduce NOx as the outflow of NOx mixing with suburban and rural areas can cause rapid PO3 growth; additionally, a continuous and consistent reduction in NOx can eventually bypass the non-linearities and make a large contribution to the reduction of PO3. Almost every city in the US used to be NOx-saturated in the late 1990s, but the steady reduction in NOx now is helping a lot at curbing PO3 and, thus, O3.

We highlight in the introduction that "NOx-saturated", "VOC-limited", and "radical limited" terminology is frequently used in the literature and are taken to have a similar meaning. Most city centers are not necessarily radical limited because VOC emissions are low, but rather because NO_x emissions are still high enough to impact OH production. A lot of our analysis and discussion focuses on the relative change in NO_x needed to transition between regimes and therefore we believe keeping the terminology related to NO_x is more appropriate in this context.

L43: Based on the EPA's report, point source emissions have decreased too. We have changed the text as follows: "*As reductions from automotive emissions and other point sources continue*"

L48. Please add additional sentences about CTM's works, observationally constrained box models, and the use of OHR to detect unmeasured VOCs with significant errors on PO3. Your introduction has brushed off a large domain of scientific endeavor.

The paragraphs at L85 & L97 discuss other approaches investigating O_3 production regimes (e.g. WD-WE effect, chemical indicators, chambers). We have modified the text at L48 as follows:

"*Alternative approaches invoke complex source apportionment or tagging methods (Wang et al., 2019; Li et al., 2023; Butler et al., 2020). Models using inventory emissions are a useful tool for O_3 source attribution as they simulate transport and photochemical processing (Abdi-Oskouei et al., 2022; Coggon et al., 2021), while simultaneously enabling sensitivity analyses that directly relate to potential emissions scenarios*"

L51. Abdi-Oskouei et al. (2022) isn't a box model study. We intended to cite Vermuel et al. (2019).

L55. Replace O3 with PO3 (ozone production rates). Replaced.

The paragraph containing 55: In both cases (NOx-sensitive and VOC-sensitive), you have radical termination either through HO2+HO2, RO2+RO2, RO2+HO2 (NOx-sensitive), or NO2+OH (VOC-sensitive). The authors need to mention the effect of RO2 and HO2 on OH formation in the presence of NO. Also, the authors need to mention that these categories (including the transitional regimes because we don't live in a binary world) are limited to photochemically active environments. Under low light conditions (radical-limited), we essentially see the portioning between NO-NO2-O3 without any noticeable effects of VOC.

In the text Sect. 4.3 we highlight that in the early morning and late evening there might be O_3 titration when we aren't in a photochemically active environment. We do not feel it is necessary to dive into a discussion involving the complex radical chemistry involving HO_2, RO_2, and OH, since the focus of this section is to give a simplified explanation of NO_x-limited versus NO_x-saturated chemistry as this is the emphasis of our further analysis. We agree there is a transitional regime, though bounding this regime is somewhat arbitrary. We chose instead to discuss everything relative to a defined transition point as described throughout the text, though we have updated Fig. 5's description to note that pale yellow coloring is where we near a transitional regime (defined as ΔNOx|transition = +/- 10%).

L69. Wasn't Jiang et al. 2019 debunked by Silvern et al. 2019? Removed Jiang et al. (2019)

The paragraph containing L95: More references need to be mentioned here about using observationally-constrained box models and using the LROx/LNOx indicator. We have added Kleinman (2005) and Rickly et al. (2023) to the five citations already listed at L85.

L99. Poor reasoning. CTMs require proper input.

We have changed the text to highlight the point we were aiming to make in that CTMs used to evaluate O_3 response are required to run multiple times at high computational costs: "*while CTMs require substantial computation time to determine the O_3 response to multiple emissions perturbations"*

Section 2.1. Where is the LiDAR measurement located? The Lidar measurement is listed in Table 1 for Pasadena site measurements and text was added to Sect. 2.1 as described earlier.

Figure 1. Please mention why you are showing D5-siloxane emissions in the caption. We have added the following text to Sect. 2.2.2 (now 2.2.3): *"Figure 1 shows an example of the spatially and time-resolved grids for D5-siloxane (a representative VCP) from FIVE-VCP-NEI17NRT"*

L162. What does a limited area version mean? This is meant to highlight it is not a global model. We have eliminated this text to avoid confusion.

L131. Dry/wet deposition? As stated in Sect. 2.2 the box model generally ignores deposition. Sect. 2.2.3 (now 2.2.4) highlights briefly that constant reaction rates are assumed for isoprene and monoterpene nitrates to account for aerosol uptake, but are not applied anywhere else.

L173. Please stick to the FLEXPART-WRF description. The F0AM part needs to be moved to another section. We updated this paragraph to only include reference to FLEXPART-WRF.

L199. Including the lockdown effect? FIVE-VCP-NEI17NRT includes near real-time (NRT) emissions to account for changes in human activity including traffic patterns as highlighted in Sect. 2.2.2 (now 2.2.3) and references therein.

L229-232. Seems irrelevant and disjointed. It is important to clarify how cooking VOCs were implemented into the model since this is the first instance it has been included in inventory work. These sentences are needed for those who want to relate this to NEI or other inventories and cities.

L294. Unclear what you mean by "limited" here. We have changed the text to read: "*The box model meteorology simplifications are challenged"*

Figure 2. Adding HCHO to these plots and discussing them in the text would be interesting, as it is a good proxy for VOCR. Section 3.3. Almost everything is included in the supplementary, which is a bit distracting. I highly suggest bringing HCHO to the discussion and the plot.

We have added HCHO to Figure 3 and have added the following text to Sect. 3.3:

"HCHO serves as a proxy for total VOCr as they are often correlated during the daytime, while the HCHO to NO_2 ratio has been used as an indicator of O_3 sensitivity (Sillman, 1995; Hong et al., 2021; Duncan et al., 2010)."

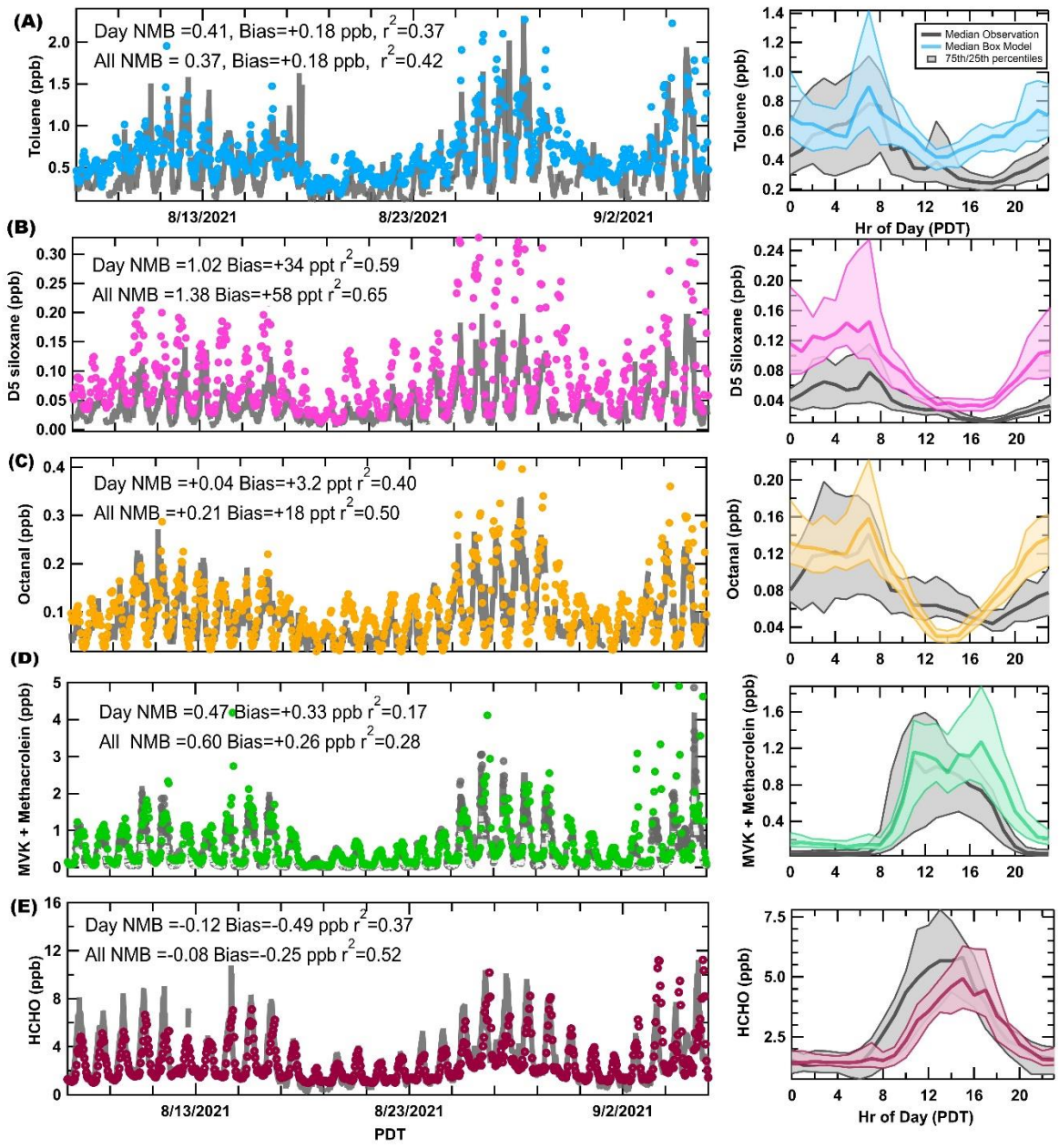

Figure 3: Left Panel: The time-series of box model output concentrations (ppb) overlaid with observations (grey lines) in Pasadena. The selected VOCs include (A) toluene (mobile sources, blue dots), (B) D5-siloxane (VCPs/personal care, pink dots), (C) octanal (cooking, orange dots), (D) methacrolein plus methyl vinyl ketone (biogenics, green dots), and (E) formaldehyde (VOCr proxy, maroon dots). Right Panel: The median diel pattern for each VOC box model output (colored) overlaid with observations (grey). Shaded regions indicate the 75th and 25th quartile ranges.

L350. R2 isn't a correlation coefficient. We have changed these instances to *"coefficient of determination"*

L403. Due to the short lifetime of isoprene, the adjustment based on MACR-MVK may not be appropriate to fully match up the isoprene concentration.

Correct. As stated in the text, even with the biogenic inventory adjustment to match the secondary products (MVK + MACR), isoprene was low compared to observations. The MVK +MACR to isoprene ratio (~0.5) also suggests the isoprene is less aged and therefore the site is heavily influenced by local emissions. For these reasons, we deemed it appropriate to scale biogenics until the oxidation products agreed with the observations rather than scaling to match isoprene observations.

L450. Do you really need to get an agreement with other studies focusing on different times and locations? I would just drop this part. You can highlight the contrasts and explain why there are some differences, but you shouldn't look for validation based on results from different environments.

We think it is important to relate to VCP contributions to anthropogenic O_3 in other major large cities and elect to keep this text.

L451. Do cooking emissions consider propane leakage? No, the cooking emissions were determined by source apportionment of VOCs measured by PTR-ToF-MS, which has low sensitivity towards alkanes.

L470. But the inflation of BVOCs wasn't enough to match up isoprene, so I'm unsure if we would call it an upper bound. We have modified the text as follows: *"It is important to note that the BVOC fraction of O_3 is estimated following a 50% increase to the prescribed BEIS BVOCs as described in Sect. 3.3*"

*L476. This is an overgeneralization. You can't statistically say this using two data points. There are indeed large spatial variances associated with photochemical conditions. If you want to include this, please expand the analysis over other sites (see the major comment).*We believe this has been addressed in previous responses. We have also updated the sentence as follows:

"Although the spatial distribution of NOx and VOCs varies basin-wide, the distribution and the magnitude of photochemically produced O3 from AVOC and BVOC does not change significantly between Pasadena and Redlands, CA"

L485. This is not true, see Tao et al. (2022) (https://doi.org/10.1021/acs.est.2c02972) and Souri et al. (2020) (https://doi.org/10.1016/j.atmosenv.2020.117341)

The intention of this sentence is to highlight other studies focus on broad regions during peak ozone production (e.g. Tao et al. (2022) in two northeastern cities) and here we are able to look at the O_3 sensitivity at different locations and times along a trajectory path. This model gives a

better understanding of the ozone sensitivity for Pasadena and Redlands and upwind of those cities. We now highlight the limitations of this approach statistically in the text.

L 487. It is an overstatement to say that a Lagrangian model can provide dense spatial information, especially relative to Eulerian frameworks. Please see our response to the major comment above.

Figure 5. This question must have been raised sooner, but which altitude do trajectories represent? Are they all within the PBL? The FLEXPART trajectories are determined after releasing particles near surface to determine what emissions are contributing most to the trajectories landing in Pasadena at the specified time. We have extensively modified the text in Sect. 2.2.1 (now 2.2.2) in response to Referee #2 to provide greater detail on the FLEXPART trajectory paths. Please see that discussion below.

Section 4.2. Is studying chemical conditions meaningful in the early morning and later afternoon when HOx-ROx is rather inactive?

Production from radicals is low in the early morning and late afternoon, so instead we generally focus our discussion on peak production periods. We state in the text: "*during early daylight hours and then decreases rapidly, allowing radical-radical reactions to compete. Although NO concentrations may be high enough to titrate O_3 during these early hours, this process is unlikely to impact O_3 response during primary production periods*"

Editorial comments

L136. 3D model retrievals -> 3D model simulations- changed

The FIVE-VCP-NEI17NRT acronym isn't easy on the eye. Can you make it more compact? This will remain as is as it is used in previous publications.

L370. What do you mean by "enhanced PBL heights"? We have changed to text to "*higher than observed PBL heights prescribed overnight by WRF-Chem*"

*L407. Formed chemically through secondary pathways…*changed

Figure 3: The color lines in the legend do not match the plots. But I don't know what the best way to fix this is. It is unclear what the Reviewer means. The Figure has been adapted to include HCHO

Figure 4. Please insert 12 ppbv somewhere in the pie plot (maybe in the middle as a text box).- changed

Line 436. Anthropogenic-induced instead of anthropogenic We elect to leave as is

*Line 478. The magnitude of photochemically produced O3 through AVOC and BVOC…*changed

Figure 5. You should clearly mention in the caption that the map is based on backward trajectories to avoid mistaking this for a continuous Eulerian framework. Because there are so rapidly elongated patterns that may seem nonsensical if we wrongly see them as separate boxes simultaneously. This figure has been adapted based on the major comment above.

Section 5. It is choppy; please break this long paragraph into smaller chunks and provide more quantitative numbers. Please provide more details about where this type of analysis, such as including cooking and VCP in PO3 sensitivity, becomes a necessity (don't limit your audience to people interested in air quality issues in LA). We have broken the Section into several paragraphs and added quantitative results to the section.

Second Referee

Note: we have re-ordered some of the Referee's comments to group similar content, making it easier to follow the discussion and avoid repetition

A Box model with updated VOC chemistry is used to determine the sensitivity of O3 to NOx and VOC emissions from various sources, including VCPs, fossil fuels, cooking, and biogenic sources, in the LA basin. FLEXPART, with input from WRF-Chem, was used to determine the trajectory of the air parcels that arrived at the two sites. Cooking emissions were added to the FIVE-VCP-NEI17NRT emission inventory and used in the box model. Various emission sensitivity experiments with the box model were conducted to assess the sensitivity of O3 concentration and MDA8 to changes in anthropogenic VOC emissions.

Key point conclusions from section 1:

- FIVE-VCP-NEI17NRT inventory shows a good representation of LA emissions in space and time when compared to O3, NOX, and speciated VOC measurements in Pasadena (I am not convinced; details below).

- They concluded that the anthropogenic VOC contributes up to 12 ppb to the total MDA8 in Pasadena (what % of the total MDA8 is this?).

Of this 12ppb:

- *44% (5.28ppb) is attributed to VCPs [5.2 +/- 0.6 ppb]*
- *28% (3.36ppb) to fossil fuel VOCs. What is the uncertainty?* see below
- *28% (3.36ppb) to cooking. What is the uncertainty?* see below

In the second part of the study, they conducted more experiments with varying NOx emissions (and VOC). They concluded that the urban core of LA basin, including Pasadena, is primarily NOx-saturated for most of the daytime and shifts to NOx-limited farther east of the LA basin.

Using an updated box model is valuable for better understanding the O3 formation and O3 regime but requires a more careful experiment setup. For example, looking at one month of simulation is typically done with a CTM, which can capture variability in the transport patterns, meteorological conditions, background O3 (and other species), etc. Box models are not typically designed to capture this type of variability.

We thank the Referee for their valuable assessment of this manuscript. We believe we have now better clarified the motivations, benefits, and limitations of using this particular box model. As discussed in our detailed response to Referee #1, our Lagrangian box model is intended as a tool to complement 3D models and enhance our understanding of the processes that impact the atmosphere. While many box models are not designed to reflect atmospheric transport, our box model accounts for transport variability driven by meteorology using 3D model inputs (FLEXPART-WRF) to derive back-trajectory air parcel paths. This approach couples accurate transport with a state-of-the-science emissions inventory to extract and react emissions along each unique path, accurately simulating O_3 across the entire campaign sampling period. Although both CTM and box model setups can have similar limitations (meteorology, boundary layer schemes, etc.), we believe our extended description demonstrates the complementary nature of the analyses and expands upon model limitations.

I see two ways to improve this work and overcome some of the limitations:

Discussions related to the back-trajectory analysis grouped together:

- *Clean up the box model input data and only include days and hours with typical transport patterns (reduce uncertainties). This may reduce the scope of the work but will significantly increase the confidence in the conclusion; L142- You described the typical transport in the LA basin and how variability in the transport pattern can introduce uncertainties. Why not only include trajectories with typical transport patterns?*

We update the text and add details below to further explain our motivation for including all days and times in this analysis. The "typical" daytime sea breeze circulation transports cooler, denser air from over water/near the coastline eastward across the LA Basin, pushing pollutants further inland. We intended to note that variability in the "traditional" transport pattern can lead to variability in the emissions that are accumulated and reacted within our model. We overcome this uncertainty by using back-trajectory analyses (FLEXPART-WRF), which enables us to capture spatial variations in emissions. We also updated all Figures and subsequent analysis to use the inputs from WRF along each trajectory to constrain to model meteorology (e.g., photolysis rates, PBLH, T, P, RH). Our new supplemental figure, described in response to the next comment, shows that the average trajectory paths during daylight hours follow the more "typical" transport that originate near the coast and transport inland.

We evaluate the model simulation with observations for daylight-only hours as well as for the full simulation (Supplemental Figure S6, now S10). We also call-out biases during peak ozone production (Section 3.1) when trajectory paths follow this more "typical transport," and obtain meaningful statistics by including all trajectories spanning an entire month. We limit our discussion of ozone responses to detailed changes to emissions at mean MDA8 O_3, which can only be calculated from the mean daily maximum 8-hour averages by not excluding any trajectories.

L170- How many air parcels were released from the site, and at what altitude? Please add a map of back-trajectories, similar to Fig S8.

Backward trajectories were calculated for twenty-five thousand particles air parcels, initialized between the surface and 20 m a.g.l, every hour from Pasadena or Redlands sites. From these 25k air parcels, FLEXPART-WRF calculates 5 clusters. The center-of-mass of the dominant cluster (i.e., accounting for the majority of the parcels) was selected as the path for the box model. This was done across the entire sampling period (7 August – 7 September), resulting in 744 trajectory paths, each (31 days x 24 hours). Coordinate locations (latitude, longitude, time) were determined every 15 minutes backwards for 4.5 hours (270 min) from Pasadena (18 coordinates / path) and 9 hours from Redlands (36 coordinates / path). Figure S2 has been added to the supplement and shows every back-trajectory path (grey dots) to each receptor site with the average backward-trajectory paths arriving hourly (24 trajectory paths, each) overlaid colored by the local time of day.

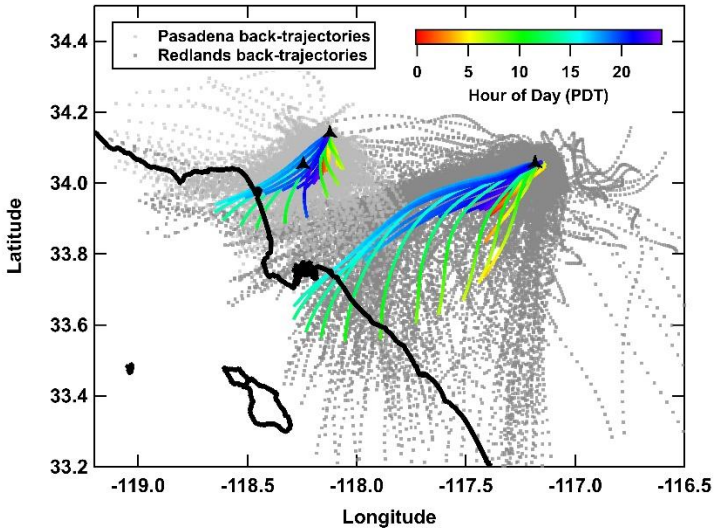

***"Figure S2:** Each series of coordinates determined at 15-minute intervals from the FLEXPART-WRF backward trajectory analysis (grey dots). Twenty-five thousand particles (air parcels) were released hourly and traced backward from both Pasadena and Redlands to determine the dominant pathway (744 trajectories, each). The average trace is shown for each hourly release time and is colored by the local time of day."*

L141- Does the location of the air parcel's starting point change for each trajectory? What do you mean by "parcel locations were derived as the center-of-mass from the main particle cluster"? What if the air particle cluster is spread?

Yes, the starting location for each air parcel arriving hourly at the receptor ground site is determined from the backward-trajectory analysis. As state above, twenty-five thousand particles are initialized at the receptor site near the surface and are traced backwards as they spread out. Rather than using the FLEXPART-WRF footprints, we use a representative location determined from the clustering algorithm by Dorling et al. (1992), implemented in the code's predecessor, FLEXPART v6.2 (Stohl et al., 2005). The advantage of this strategy is the explicit representation of turbulence in FLEXPART-WRF, which affects the localization of the emerging clusters. Coordinates are determined every 15 minutes, representing the center-of-mass (the densest portion) of the main cluster of particles. A series of trajectory paths is shown in Supplemental Fig. S8 (now S13) and the added Supplemental Figure S2, which includes all trajectory coordinates and averaged hourly paths. We have reworded the FLEXPART-WRF description in Section. 2.2.1 as follows:

"*The model calculates particle dispersion backwards, releasing twenty-five thousand particles (air parcels) between the surface and 20 m above ground level. For particle masses released hourly in FLEXPART-WRF, trajectories were followed back for 18 hours. To simulate the trajectory of air parcels arriving hourly, coordinates (latitude, longitude, altitude) were derived every 15-minutes as the center-of-mass of the main particle cluster. Ancillary information (photolysis rates, boundary layer height, temperature, pressure, relative humidity) was obtained at each coordinate from 4–D interpolation along each trajectory from the WRF model coupled with chemistry (WRF-Chem) (Grell et al., 2005) completed for SUNVEx campaign period (Zhu et al., 2024a). More information about the WRF-Chem setup can be found in Zhu et al. (2024a)"*

L148- "emissions encompassed by the area of the box…". To clarify, the box moves based on the back-trajectory information. You then extract the emission rates from the inventory for that given lat/lon (8x8km box) and add that to equation 1?

Yes, the FLEXPART-WRF analysis provides estimated paths that consider meteorology. Coordinates (latitude, longitude, time) were determined every 15 minutes, for 744 different trajectory paths to each receptor site. Time- and location-varying emissions are extracted at each coordinate bounded by a defined box area (8 x 8 km). The updated description at the start of Section 2.2 (now Sect. 2.2.1), the new Supplemental Fig. S1 showing a generic representation of Lagrangian box models added in response to Referee #1, and a new Supplemental Fig. S2 clarify this setup.

L149- Is PBLH assumed to be the same throughout the trajectory as the measured values at the Pasadena site? Line 151 says observations and 3D-model estimates constrain the PBL. Which observation? Where model estimates are used? Again, very critical information is missing. Is this a reasonable assumption?

As detailed in response to Referee #1, we have updated the model simulation to use meteorology (temperature, pressure, relative humidity) and PBLH from WRF-Chem along each trajectory path

and constrain to measurements only at the Pasadena site. These parameters change spatially and temporally and are set to true observations at the end point.

If you decide to run WRF-Chem for this study, you can use the trajectory monitoring feature in WRF-Chem and skip using FLEXPART. See here for details:
https://www2.acom.ucar.edu/sites/default/files/documents/Trajectory.desc_.pdf
With FLEXPART, you can easily create an ensemble run of air parcels and quantify transport uncertainties.
Thanks for the recommendation about the trajectory monitoring feature in WRF-Chem. We will look into this for future work. Our responses above describe our motivation for coupling this analysis with FLEXPART-WRF to accurately simulate air parcel pathways.

L180- Another reason to only include certain hours (mid-day with filly developed boundary later) in the analysis.

We acknowledge the Referee's point about focusing on mid-day hours when the boundary layer is fully developed. However, for reasons detailed earlier, we elected to include all trajectories in this analysis and the updated Fig. S2 shows that the average trajectory paths arriving midday (during peak production), which most of our analysis focuses on, originate near the coast and transports inland.

Discussions related to a companion CTM analysis and inventory emissions grouped together:

- *Add CTM analysis to complement this study. In my opinion, adding a CTM analysis, especially to evaluate the performance of the new emission inventory, is essential.*

Our box model complements the work conducted by Zhu et al. (2024a), which describes a WRF-Chem analysis for the LA Basin during the same 2021 SUNVEx campaign. The CTM model is configured with the FIVE-VCP-NEI17RT inventory and used a similar reduced chemical mechanism scheme (RACM2B-VCP). We have added a paragraph to Sect. 2.2 to direct the reader to the WRF-Chem analysis previously published. FIVE-VCP-NEI17RT has been extensively evaluated in previous studies (McDonald et al., 2018b; Coggon et al., 2021; He et al., 2024; Kim et al., 2022; Zhu et al., 2024a; Zhu et al., 2024b; Harkins et al., 2021; Pfannerstill et al., 2023; McDonald et al., 2012) as well as in LA during SUNVEx as described by Zhu et al. (2024a). A primary difference is that cooking VOC emissions were added for this analysis. These emissions are also included in an updated WRF-Chem simulation in a recently submitted manuscript (Zhu et al., 2024b). The WRF simulated cooking VOCs are evaluated with observations at the Pasadena site using the same cooking VOC tracers discussed in this manuscript (octanal, nonanal); thus, these cooking updates are essentially validated by our observations. Section 3.1 reports the NMB and R^2 in Pasadena for both the box and 3D model simulated O_3.

The following is the added paragraph to Sect. 2.2.: *"The box model is designed to complement the Weather Research and Forecasting model coupled with Chemistry (WRF-Chem) model simulations described by (Zhu et al., 2024a), which was configured using anthropogenic emissions from the FIVEVCP-NEI17NRT inventory and an updated chemical mechanism named RACM2B-VCP. The WRF-Chem model accurately reproduced O_3 and many speciated VOCs across the LA*

Basin during the summer of 2021. The box model in this study leverages the WRF-Chem output to constrain transport and meteorological variability (see Sect. 2.2.2) and is configured with the same emissions (see Sect. 2.2.3) and chemistry (see Sect. 2.2.4) described by (Zhu et al., 2024a), with modifications detailed in the following subsections. The box model is intended to evaluate O_3 responses to emissions perturbations and to asses sector contributions to photochemical O_3 observed at two receptor sites. The model can also be used for mechanism development, which is challenging to perform in CTMs. Here, we focus on describing the model and corresponding O_3 responses to anthropogenic VOC and NO_x perturbations."

L165- Verreyken et al. (2024) paper is in prep. Please add information regarding the WRF-Chem performance in capturing transport in this paper.

The FLEXible PARTicle dispersion model (FLEXPART) is a widely used Lagrangian particle dispersion model for simulating atmospheric transport processes. Details of the FLEXPART-WRF configuration are described in Sect. 2.2.1 (now 2.2.2), which uses hourly average winds to reduce uncertainty and bias of the model in complex terrain (Brioude et al., 2013). Moreover, recent studies by Karion et al. (2019) and Angevine et al. (2020) discussing uncertainty in Lagrangian transport models have been considered to further reduce the uncertainty in the transport model. Karion et al. (2019) highlights independent vertical mixing parameterizations in Lagrangian transport models as a cause for divergence between their inversion results. To address this, the Verreyken et al. (2019) implementation of vertical turbulence was used in FLEXPART-WRF for a consistent treatment of vertical turbulence between the meteorological model and the transport model. Angevine et al. (2020) highlights the performance of the meteorological model used to calculate trajectories as a primary source of uncertainties. To take this into consideration, Verreyken et al. (2024, under review) have run the WRF model using different configurations and select the optimum by comparing vertical wind profiles in the model to those obtained from a Pick-Up truck based Mobile Atmospheric Sounder (PUMAS) strategically deployed in the LA basin during the SUNVEx campaign. This work has recently started the peer review process but will likely not be publicly available before this manuscript.

L303- "the general agreement…" Drawing this conclusion from only NMB and R2 is not accurate. Can you compare O3 and NOX concentrations between the box model and WRF-Chem along the trajectory and at the site?

We respectively argue that validating the model simulations with real-world observations is more valuable than comparing to another model to assess the accuracy in predicting actual concentrations. While ground-site observations might be impacted by local sources, we show that comparing hourly observations to the model demonstrates good agreement. Many modeling studies rely on NMB calculations and statistical analyses such as R^2 when evaluating the accuracy of model simulations. The box model shows similar NMB and R^2 values to those reported in Zhu et al. (2024a).

2.2. Emissions A lot of important information is missing from this section.

So, if there are mismatches in the location of emissions, will they not be added correctly to the box model? If this is true, then this is another important limitation of this work. This points out the importance of evaluating the new emission inventory using CTM prior to running box models.

This Lagrangian box model considers varied transport using the backward trajectory analysis. This analysis accounts for meteorology and is meant to inform the spatial and temporal variability in emissions from the surface contributing to the air mass that eventually arrives at the receptor site. Only emissions at each defined coordinate (latitude, longitude) are fed into each box volume at the defined time interval as parcels transport across the basin. The complementary CTM analysis (Zhu et al., 2024a) was evaluated with surface sites, mobile measurements, and aircraft measurements across the entire LA Basin and suggests that the spatial distribution of the emissions inventory accurately represents reality based on the good agreement with observations across several sampling platforms. The box model agreement with observations for O_3, NO_x, and VOCs also suggest that the emissions extracted along each trajectory and chemical reactions reasonably represent atmospheric processing.

Please add details about the diurnal variability of emissions from each sector (can be a diel plot).

There are other publications that have used and detailed the anthropogenic emissions inventory used in this work, which includes its various generations: FIVE inventory, FIVE coupled with anthropogenic VCPs (FIVE-VCP), and FIVE updated to reflect near-real time emissions (FIVE-VCP-NEI17NRT). We have directed the reader to the detailed description in the supplement of He et al. (2024) and have added the following text to Sect. 2.2.2 (now 2.2.3).:

"*The diel emission profiles from FIVE for on-road emissions are detailed in McDonald et al. (2014), while those for off-road emissions are found in McDonald et al. (2018a) with updates to marine gasoline provided by Yu et al. (2023). Most VCP diel profiles are sourced from the EPA National Emissions Inventory (NEI) 2014, version 2, with personal care updated to reflect the emissions of D5-siloxane as outlined by Coggon et al. (2018). Temporal profiles for other sources were taken from the 2017 NEI (https://gaftp.epa.gov/air/emismod/2017).*"

More details on the cooking temporal profile were also added to Sect. 2.2.2 (now 2.2.3) as well as supplemental Fig. S4: "*A temporal profile representing human activity was taken from the commercial cooking profile used in the 2017 NEI (Supplemental Fig. S3).*"

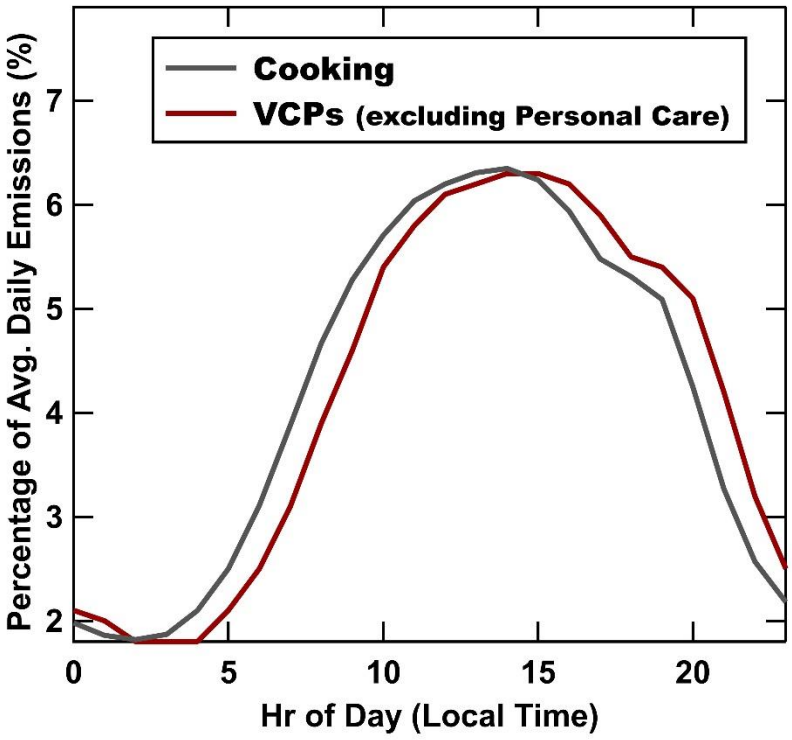

Figure S3: *The temporal profile of cooking and VCP emissions as a percentage of average daily emissions used in the FIVE-VCP-NEI17NRT inventory. The cooking profile is taken from the 2017 National Emissions Inventory (NEI) commercial cooking temporal profile (code 26).*

Fig1. I highly suggest adding maps of emissions by sector in the paper or in SI.

Figure 1 is meant to show an example of the 4 × 4 km spatially gridded emissions from the hourly FIVE-VCP-NEI17NRT emissions inventory for a single VOC (D5-siloxane) at a select time. The sector emissions vary by location (lat,lon), time of day, weekday vs weekend, and by species. The temporal and spatial variability cannot be simplified into a Figure. The emission files are available for download (https://csl.noaa.gov/groups/csl7/measurements/2021sunvex/emissions/) and a detailed description of FIVE-VCP-NEI17NRT emissions is outlined in the supplement of (He et al., 2024).

Please add details about the spatial variability of emissions from each sector (it can be a map), especially the cooking sector. How are population density and temporal profile for human activity used for the spatial distribution of cooking emissions?

We provide a detailed description of how cooking VOCs were determined by source apportionment in Sect. 2.2.2 (now 2.2.3) using VOC measurements in Las Vegas. These VOCs were then spatially distributed based on population density and temporally distributed using a temporal profile for human activity as described above. We have added a table to the Supplement showing the speciation (mass fraction from PMF) and mechanism mapping for cooking inventory VOCs along with the temporal pattern of cooking as described above.

Species	Formula	WRF	RACM2B-VCP	Mass Fraction (base)	Mass Fraction (upper EOH)
Acetaldehyde	C2H4O	HC15	ACD	0.068	0.043
Ethanol	C2H6O	HC48	EOH	0.130	0.449
Acrolein	C3H4O	HC27	CUALD	0.006	0.004
Acetone / propanal	C3H6O	HC18	ACT	0.075	0.048
Acetic acid	C2H4O2	HC31	ORA2	0.068	0.043
Butenal	C4H6O	HC67	CUALD	0.006	0.004
Propanoic acid	C3H6O2	HC32	ORA2	0.011	0.007
Pentadienal	C5H6O	HC46	DIEN	0.039	0.024
Butenedial	C4H4O2	HC67	CUALD	0.004	0.002
Pentenal	C5H10O	HC67	CUALD	0.041	0.026
Pentanal	C5H10O	HC62	CALD	0.037	0.024
Buytrolactone	C4H6O2	HC20	KET	0.014	0.009
Hexadienal	C6H8O	HC46	DIEN	0.042	0.027
Pentanoic acid	C5H10O2	HC32	ORA2	0.004	0.002
Heptadienal	C7H10O	HC46	DIEN	0.004	0.003
Heptenal	C7H12O	HC67	CUALD	0.009	0.006
Heptanal	C7H14O	HC64	CALD	0.013	0.008
Octadienal	C8H12O	HC46	DIEN	0.013	0.008
Octenal	C8H14O	HC67	CUALD	0.011	0.007
Octanal	C8H16O	HC65	OALD	0.019	0.012
Heptanoic acid	C7H14O2	HC32	ORA2	0.001	0.000
Monoterpene	C10H16	HC11	0.5*LIM+0.5*API	0.010	0.006
Nondienal	C9H14O	HC46	DIEN	0.009	0.006
Nonenal	C9H16O	HC67	CUALD	0.004	0.002
Nonanal	C9H18O	HC66	NALD	0.020	0.013
Octanoicacid	C8H16O2	HC32	ORA2	0.002	0.002
Decatrienal	C10H14O	HC46	DIEN	0.014	0.009
Decadienal	C10H16O	HC46	DIEN	0.012	0.007
Decenal	C10H18O	HC67	CUALD	0.003	0.002
Decanal	C10H20O	HC68	CALD	0.004	0.003
Nonanoicacid	C9H18O2	HC32	ORA2	0.001	0.001
Undecenal	C11H22O	HC67	CUALD	0.001	0.001
Undecanal	C11H20O	HC68	CALD	0.002	0.001
Decenoicacid	C10H18O2	HC08	OLT	0.002	0.001
Decanoicacid	C10H20O2	HC32	ORA2	0.001	0.000
Tridecanal	C13H26O	HC68	CALD	0.002	0.001
Furfural	C5H4O2	HC68	CALD	0.005	0.003
C7H8O2	C7H8O2	HC32	ORA2	0.005	0.003
Benzaldehyde	C7H6O	HC17	BALD	0.004	0.003
C6H8O2	C6H8O2	HC32	ORA2	0.004	0.003

C6H10O2	C6H10O2	HC32	ORA2	0.016	0.010
C8H1002	C8H1002	HC32	ORA2	0.003	0.002
C8H12O2	C8H12O2	HC32	ORA2	0.003	0.002
C8H14O2	C8H14O2	HC32	ORA2	0.006	0.004
C9H14O2	C9H14O2	HC32	ORA2	0.002	0.001
C9H16O2	C9H16O2	HC32	ORA2	0.002	0.002
Unspeciated	NA	HC06	HC8	0.249	0.158

Table S1: *The cooking speciation profile (mass fraction) determined by Coggon et al. (2024) mapped to the RACM2B-VCP mechanism.*

Have the cooking emissions been evaluated in any CTM model? If not, how does this limit your conclusions?

Cooking VOC emissions were incorporated into the FIVE-VCP-NEI17NRT inventory that was run within the complementary WRF-Chem simulation that was recently submitted by Zhu et al. (2024b). They compare the CTM simulation using NMB and R^2 for aircraft, mobile, and site measurements in Pasadena for cooking tracers, with the nonanal NMB being -0.41, -0.42, -0.12, respectively. This evaluation does not differ significantly from our evaluation using NMB and R^2 at the same ground site as shown in Figure S6 (now S10). Zhu et al. (2024b) also shows how including cooking VOCs in the total VOC OH reactivity improved agreement with observations for overlapping VOCs.

Where are oil and gas emissions? Part of fossil fuel? Low ethane concentrations in the model compared to observation. Did you include oil and gas emissions in your study? Is it part of fossil fuel emissions?

In Section 2.2.2 (now 2.2.3) we state: "*The fossil fuel sectors comprise diesel exhaust, evaporative gasoline, gasoline exhaust, off-road diesel and gas, commercial marine vessel, powerplant, and fuel-based oil and gas emissions.*" We have also cited the supplement of He et al. (2024) for a more thorough description of the emissions inventory.

L576 Why FIVE-VCP has 50% lower off-road VOCs?

It is beyond the scope of this manuscript to investigate the detailed differences between various anthropogenic emissions inventories. As detailed in Sect. 2.2.2 (now 2.2.3) both on-road and off-road engine sources are from the Fuel-Based Inventory of Vehicle Emissions (FIVE) and are updated using fuel sales. The CEPAM tool uses a specific Off-Road Mobile Source Emissions Inventory (https://ww2.arb.ca.gov/msei-road-documentation). The pie charts in Fig. S9 (now S16) show the differences in the distribution of VOC emissions by source sector between CARB CEPAM2019v1.03 and FIVE-VCP-NEI17NRT anthropogenic inventories.

Discussions related to the Model configuration grouped*:*

2.1. Campaign description

You mentioned that the trailer was away from Aug 2-6 and then from Aug 31 to Sep 3. Fig 2a, shows measurements until Sep 6th. Was Sep 3-6 was included in the study? Fig 2. You can exclude days after Sep 3rd if VOC obs is not available then?

Several hours were missing when the mobile laboratory was away from the site on those days. On-site setup occurred from Aug 2-6, resulting in an incomplete observational data set for these days, which were therefore excluded from the analysis. Onboard measurements for missing hours from Aug 31-Sep 3, which were primarily VOCs from the PTR-ToF-MS, were also excluded from the NMB and R^2 analysis. Other on-site measurements, such as O_3, were measured continuously, allowing the comparisons in Fig. 2A to span the entire month. This clarification has been added to the text in two locations.

"*The mobile laboratory was deployed to characterize the spatial distribution and to determine the local sources of emissions for times within two periods (2–6 August; 31 August – 3 September 2021). Onboard measurements during hours when the mobile laboratory was away from the ground site were excluded from this analysis*."

"*For comparisons with ground-site observations VOC measurements were excluded when the mobile laboratory conducted drives (during times between 31 August – 3 September).*"

2.2. Box model configuration

L147- How are the initial mixing ratios determined? This is an important piece of information that is missing from the text. There is a mention of ozone concentrations being initialized using measurements from the Westchester SCAQMD site during the day (why not at night?) in section 2.2.4. Is this used for all the trajectories? This site is next to LAX (major pollutant source); how does this impact your conclusions? If the initialization is done using WRF-Chem values, how is the performance of this model? In general, how sensitive are your conclusions to the initial values you pick for your box model? L284- How exactly are the measurements from the Westchester site used? Please mark it on the map in Fig 1.

The description at the beginning of Sect. 2.2 (now Sect. 2.2.1) provides a general overview of the model configuration, with more explicit details given in subsequent sections. In the general overview, much of the text has been reorganized, as well as a slight reorganization for several sections in Sect. 2.

Box models can be initialized with observational data, predefined initial conditions based on historical data, or assumed mixing ratios. In this study, we elect to initialize each trajectory with O_3 concentrations measured hourly from the Westchester SCAQMD (LAX) air monitoring site, which is the closest AQS site along the trajectory path near the coastline. Based on average trajectory paths to Pasadena (new Fig. S2), it is assumed that parcels are generally initialized over the water or near the coast. Constraining to observations better captures real-world O_3 variability and helps account for photochemically produced O_3 as the day progresses. At night, O_3 concentrations generally stabilize with limited photochemical production, but O_3 titration might

occur as the boundary layer collapses and is further complicated as O_3 accumulates in a residual layer. The SCAQMD site was added to Figure 1 (labeled LAX) and the O_3 time series and diel for this site was added to the supplement, which was used for the initial O_3 mixing ratios.

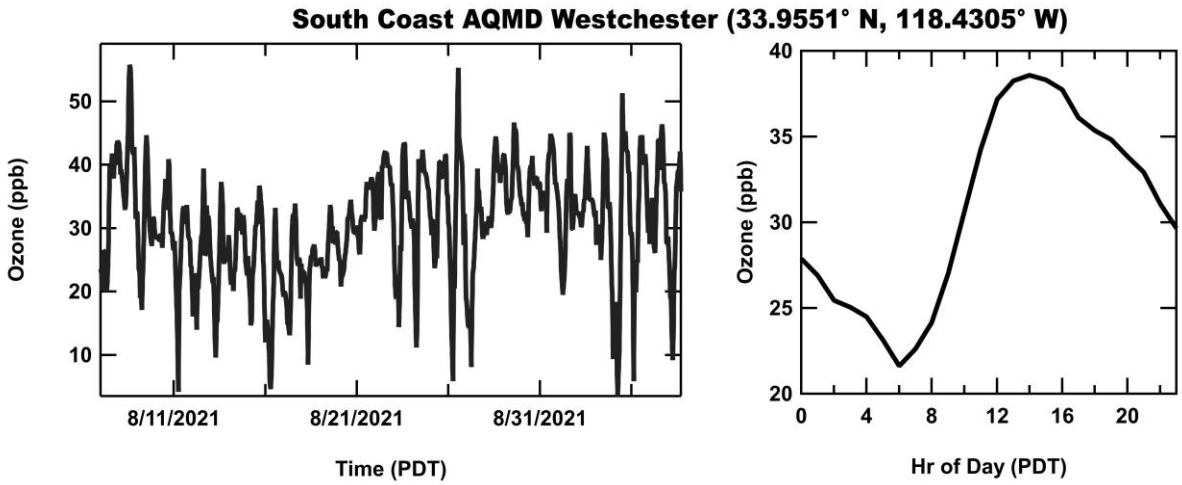

Figure S5: The O_3 time-series and diel profile from the South Coast Air Quality Management District (SCAQMD) Westchester site (33.9551° N, 118.4305° W) used as the initial O_3 mixing ratios in the model.

A sensitivity analysis shows that holding the initial O_3 mixing ratio constant affects the absolute total MDA8 O_3, but does not significantly impact the contribution of emission sector VOCs to anthropogenic MDA8 O_3 (less than 1% difference). Thus, most of the discussion focuses on the fractional distributions of AVOC MDA8 O_3 and absolute AVOC MDA8 O_3 and we do not discuss the fractional contribution to total MDA8 O_3.

Fig 3. X-axis label is not correct. This Figure has been updated.

Formaldehyde matches observation well. Give the low bias in isoprene, probably for the wrong reasons.

The biogenics were scaled up to match the first-generation oxidative products of isoprene. Isoprene was still underestimated when compared to observations and we attribute this to local vegetation at the ground site as detailed in response to Referee #1. Other box models in the region have tried to constrain BVOCs using observations, and found they also needed to scale down observations since the modeled BVOC secondary species (HCHO, MVK, MACR) were originally too high (Chen et al., 2024).

Discussions related to the Sensitivity Analyses grouped:

4.1. Contribution of Anthro and bio VOCs to O3

In my opinion, to correctly capture the impact of all the anthropogenic sectors, you need to run a scenario with all anthropogenic emissions removed instead of using Equation 4. Same goes with 10% reduction.

This study investigates ozone responses to detailed changes to emissions and chemical mechanisms using a similar approach to those applied previously (e.g. Coggon et al. 2021). We estimate the relative change in MDA8 O_3 by zeroing anthropogenic VOCs from each source sector. Summing the relative changes resulting from all source sector VOCs gives the total AVOC and sector-specific AVOC O_3 contributions, calculated at the mean daily maximum 8-hour average (MDA8) O_3 for the entire month of sampling (Eq. 4). We have updated the text as follows to clarify that this represents the relative contribution of VOCs from each emission sector to the total AVOC O_3 calculated at MDA8 O_3.

"*The change in MDA8 O_3 from anthropogenic VOCs in each emission sector in the FIVE-VCP-NEI17NRT inventory was summed to estimate the total O_3 from anthropogenic VOCs (termed "AVOC ozone") following Eq. (4).*

"*The pie chart in Fig. 4A shows the source sector AVOC O_3 contributions determined at MDA8 O_3*"

An advantage of this box model is its ability to invoke small incremental changes to evaluate response, minimizing the risk of altering photochemical regimes with large changes to bulk VOCs or NO_x. Figures 5 and 6 show that even small changes in NO_x and VOCs can alter photochemical regimes. The pie chart in Figure 4 describes AVOC contributions to AVOC MDA8 O_3 and can only be generated by turning off VOCs specific to each emissions sector. It is also worth noting there are no NO_x emissions prescribed by the inventory for VCPs or cooking, and a primary focus of this manuscript is the impact of these particular source sectors.

Another point: In reality, you cannot turn off some pollutants from a sector (only VOCs, not NOX) and asses the contribution of this sector on O3 concentration/production or MDA8. As you mentioned, the system is non-linear; thus, including both VOC and NOx simultaneously matters. Changes in the O3 chemical regime are part of the reality and need to be studied.

4.2. Spatial and temporal ozone sensitivity to NOx. Similar to scenarios in the previous section, preturbing only NOx does not show us the full picture of the impact of mitigation policies on O3 concentrations

We agree with the Referee that the O_3 response to changing VOCs and NO_x is much more complex in the real-world, and regulatory restrictions might target specific VOCs plus NO_x from particular source sectors (e.g. automotive gasoline or diesel). However, it is common to investigate the impact of bulk NO_x or VOC reductions on O_3 response, as we have done here, to help identify specific impacts and enables a more comprehensive understanding of air quality management approaches. In this manuscript, we emphasize a focus on anthropogenic VOC contributions to O_3 and do not investigate the contributions of anthropogenic NO_x plus VOCs. The analysis in Sect. 4.2 does focus on response to bulk changes to NO_x, without specifically targeting any one emission sector. Sect. 4.3 evaluates how differing VOCs represented by various anthropogenic emissions inventories impact those conclusions. The companion WRF-Chem analysis recently submitted (Zhu et al. (2024b)) investigates the impact of electrification assuming reductions to on-road gasoline NO_x and VOCs emissions, but this same analysis is not the focus of this manuscript.

L435:Can you add details about the variability and standard deviation of the data? How many ppb is 28%?

We have now updated our values to show the average +/- standard deviation of the daily maximum 8-hour moving average O_3 (MDA8 O_3) measured over the entire month of sampling (7 Aug – 7 Sept). We have also added the absolute average ± standard deviation in parentheses for each sector AVOC O_3 contribution in the main text.

"*Supplemental Figure S2 shows the O_3 diel profile for the 8-hour moving average during the sampling period and the average ± standard deviation MDA8 O_3 from the model (59.5 ± 7.2 ppb) compared well with observations (60.4 ± 13.3 ppb) in Pasadena*"

L437:Coggon et al showed fossil fuels contribution to ozone production from AVOC at midday was 60%. This is different from the 28% contribution to MDA8 ozone in this work. Please be more precise about your conclusions in this paragraph.

We have clarified in the text that the fossil fuels contribute 29% to the AVOC O_3, whereas Coggon et al. (2021) showed that fossil fuels accounted for 60% of the AVOC O_3 in NYC at midday for an exceedance event.

"The distribution shows that AVOCs from VCP sectors account for 45% (5.8 ± 1.3 ppb) of the mean AVOC MDA8 O3 while fossil fuels including other area emissions account for 29% (3.8 ± 0.8 ppb). In contrast, Coggon et al. (2021) showed fossil fuels were 60% of the AVOC O3 in NYC midday during an exceedance event.

What is the total mass of VOC and NOX emissions in each city? Is fossil fuel emission lower in LA?

Fig. S7 of Coggon et al. (2021) shows Fossil Fuels (FFs) were approximately 40% and VCPs ~60% of the VOC distribution in Manhattan in 2021, while cooking emissions were not included in that study. Conversely, our Fig. S9 (now S14) shows that in SoCAB, FFs are a much smaller fraction, while VCPs are still ~60% of the VOCs. For NO_x, we re-extracted emission rates (t day^{-1}) in Manhattan, NY and compare to the entire South Coast Air Basin of LA (shown below). As expected the total emission rate for the area of Manhattan (38 t/day) is much smaller that the SOCAB (270 t/day). There is a contribution from oil and gas (O&G) in LA, while both on-road and non-road engines contribute more significantly in LA than they did in NYC.

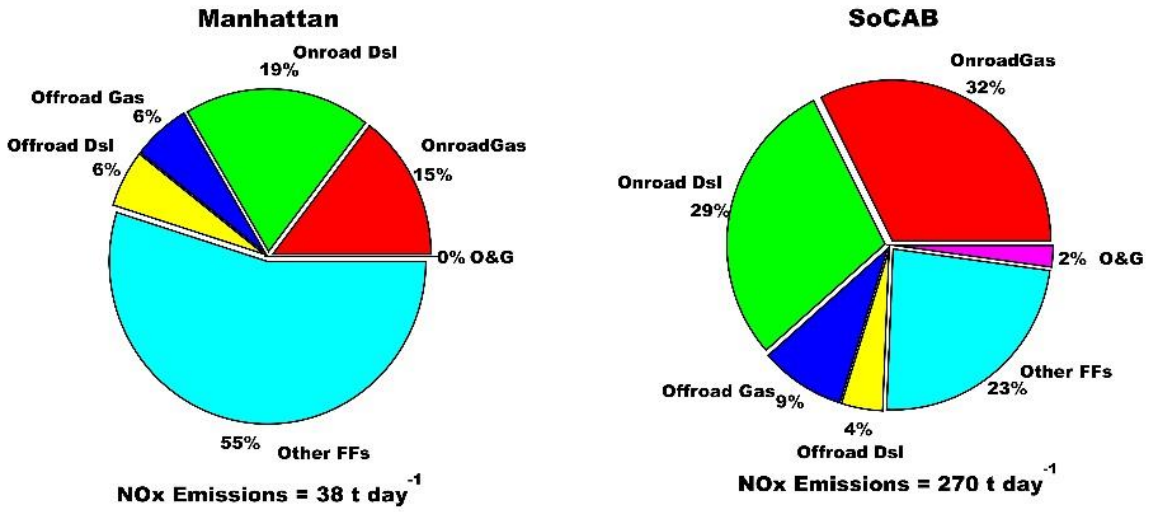

L453:What is the contribution of each sector to OH reactivity? Adding more details on this can be valuable for the discussion.

We have now added a pie chart showing the VOC OH reactivity determined from the anthropogenic emissions input into the model by emission sector averaged from 12:00-15:00 LT to the supplement.

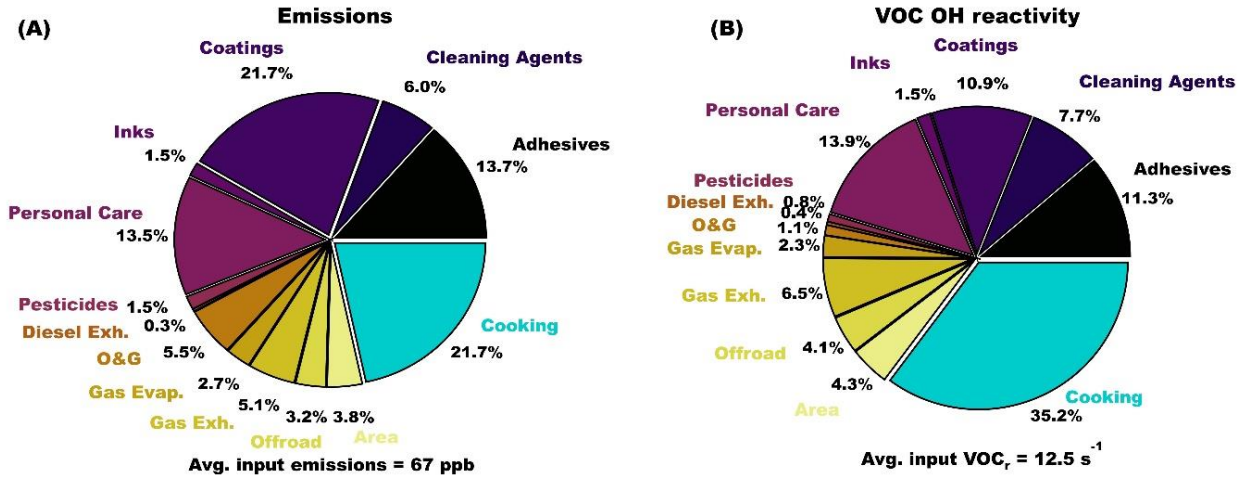

Figure S10 *(A) The distribution of anthropogenic (A) VOC emissions and (B) VOC OH reactivity by emission source sector input into the model, averaged for arrival times in Pasadena between 12:00-15:00 LT.*

To draw a more comprehensive conclusion about the NOx vs VOC sensitivity in the region, you can use metrics such as FNR, LROx/LNOx, or methods as described in Vermeuel et al. 2019(https://doi.org/10.1029/2019JD030842) (they also used a box model). Box models can provide details about PO3, OH reactivity, etc. Please use this information in your discussion about the O3 regime.

At the suggestion of the Referee, instead of evaluating the absolute ozone mixing ratio response to NO_x in Figure 6, we instead evaluate both the mean MDA8 O_3 and the mean MDA8 net ozone production rate (PO_3), defined as the difference between the instantaneous rate of O_3 formation and destruction. MDA8 O_3 is used by regulatory agencies, while PO_3 represents a net production rate (ppb/hr) that might be less impacted physical processes including O_3 accumulation. The rate of formation here is approximated as the sum of reactions that convert NO to NO_2, which includes all rates of reactions between peroxy radicals and NO (HO_2+NO and all RO_2+NO reactions). The rate of destruction includes the reaction of O_3 photolysis and the subsequent reaction of O1D with water vapor, reactions of O_3 with OH, HO_2, and alkenes, and the formation of HNO_3 by the reaction of OH with NO_2.This is now summarized in the new Supplementary Eq. (S1).

The motivation for using MDA8 O_3 (ppb) instead of absolute O_3 (ppb) is that it is commonly used as a key metric to assess compliance with NAAQS and it eliminates the time-of-day biases that might arise when only averaging trajectories that arrive at 14:00 LT, which we had used in the previous iteration of Fig. 6. Alternatively, net ozone production rates (PO_3, ppb h^{-1}) are a measure of how much ozone is being produced and is tied directly to chemical processing and might be less impacted by transport and mixing of background ozone. The Figure below, shows that the mean MDA8 O_3 and mean MDA8 PO_3 versus NOx scaling curves are very similar for the base case simulation. Supplemental Fig. S15 and Eq. (S1) were added to the supplement and show the MDA8 PO_3 vs NOx curves follow the same trends as Fig. 6.

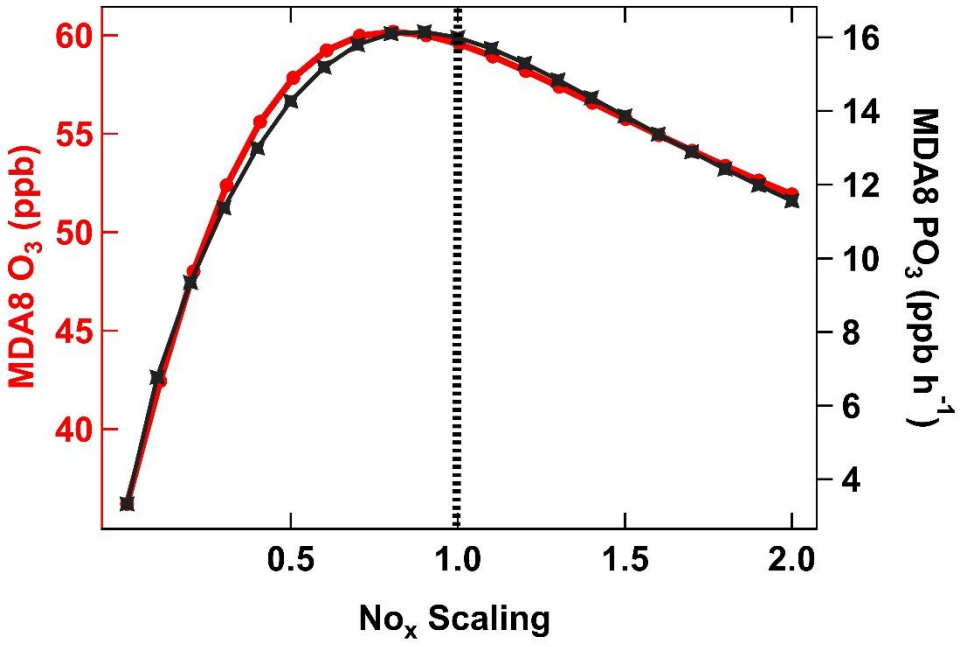

$$PO_3 = k_{HO_2+NO}[HO_2][NO] + \sum_i k_{RO_{2_i}+NO}[RO_{2_i}][NO] - k_{O1D+H_2O}[O1D][H_2O] - k_{OH+NO_2}[OH][NO_2] - k_{HO_2+O_3}[HO_2][O_3] - k_{OH+O_3}[OH][O_3] - k_{alkenes+O_3}[Alkenes][O_3]$$

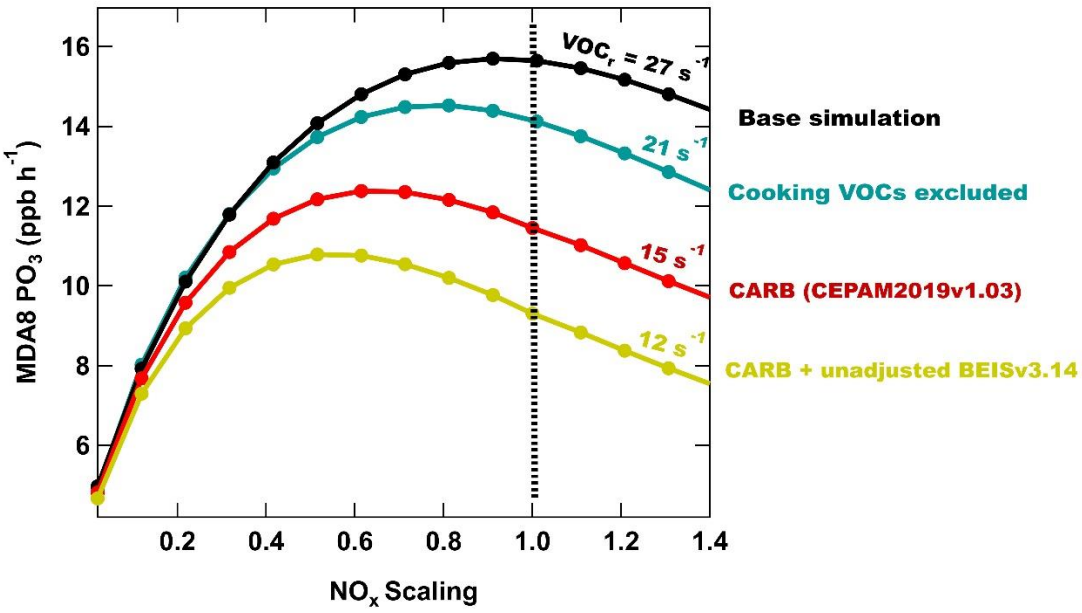

Figure S13. *The change in the campaign average MDA8 ozone production rate (PO3) as NOx is scaled from its initial mixing ratio (dashed line) for the following scenarios: (1) Base model simulations. (2) Base emissions excluding cooking VOCs (blue). (3) emissions where VOCs were adjusted to better match the CARB-CEPAM inventory emissions (red). (4) Scenario 3 with BVOCs scaled down to match the original BVOCs prescribed by the BEIS inventory coupled with WRF-Chem (yellow). PO_3 is defined by Supplemental Eq. (S1).*

Changes in MDA8 ozone mixing ratios are critical for assessing the impacts of NO_x on air quality and emissions control. As outlined in the introduction, there are alternative approaches to investigating instantaneous NO_x sensitivity and determining ozone photochemical regimes using models or observational data. These include the HCHO to NO_2 ratio, measured/simulated radical production and loss using various parameters (e.g. H_2O_2/HNO_3 or Ln/Q), WD-WE effect, chambers O_3 response, etc. Each method has its advantages and disadvantages, though evaluating all of these indicators is beyond the scope of this manuscript.

Figure 6. A better comparison is the Red scenario + cooking emission.

Figure 6 is intended to investigate O_3 response to NO_x for VOCs represented by different anthropogenic emission inventories. Other studies, including this one, indicate Pasadena is near the transitional regime and sits close to the urban core of LA, where changes to emissions can have critical impacts. Therefore, the inclusion of cooking VOCs affects NO_x and VOC–control assessments at that specific location in the basin. We believe using Pasadena for sensitivity analyses is more pertinent than in Redlands, which generally sits definitively in the NO_x sensitive regime much further inland.

This paper contains many missing details and contradictory conclusions. I tried my best to understand and guess some of the assumptions by reading the references and going back and forth in the paper many times. I highly recommend reorganizing the paper and adding more information and details about the methods, assumptions, and, most importantly, limitations of this study. We

believe the updates have improved the organization and flow of the manuscript, with a particular focus on Section 2.2.

3. Model evaluation: I wish the method section had more details so I could review sections 3, 4, and 5 more thoroughly.

Thank you, and good luck!

References

Abdi-Oskouei, M., Roozitalab, B., Stanier, C. O., Christiansen, M., Pfister, G., Pierce, R. B., McDonald, B. C., Adelman, Z., Janseen, M., Dickens, A. F., and Carmichael, G. R.: The Impact of Volatile Chemical Products, Other VOCs, and NOx on Peak Ozone in the Lake Michigan Region, Journal of Geophysical Research: Atmospheres, 127, e2022JD037042, https://doi.org/10.1029/2022JD037042, 2022.

Angevine, W. M., Peischl, J., Crawford, A., Loughner, C. P., Pollack, I. B., and Thompson, C. R.: Errors in top-down estimates of emissions using a known source, Atmos. Chem. Phys., 20, 11855-11868, 10.5194/acp-20-11855-2020, 2020.

Brioude, J., Arnold, D., Stohl, A., Cassiani, M., Morton, D., Seibert, P., Angevine, W., Evan, S., Dingwell, A., Fast, J. D., Easter, R. C., Pisso, I., Burkhart, J., and Wotawa, G.: The Lagrangian particle dispersion model FLEXPART-WRF version 3.1, Geosci. Model Dev., 6, 1889-1904, 10.5194/gmd-6-1889-2013, 2013.

Butler, T., Lupascu, A., and Nalam, A.: Attribution of ground-level ozone to anthropogenic and natural sources of nitrogen oxides and reactive carbon in a global chemical transport model, Atmos. Chem. Phys., 20, 10707-10731, 10.5194/acp-20-10707-2020, 2020.

Chen, T., Gilman, J., Kim, S.-W., Lefer, B., Washenfelder, R., Young, C. J., Rappenglueck, B., Stevens, P. S., Veres, P. R., Xue, L., and de Gouw, J.: Modeling the Impacts of Volatile Chemical Product Emissions on Atmospheric Photochemistry and Ozone Formation in Los Angeles, Journal of Geophysical Research: Atmospheres, 129, e2024JD040743, https://doi.org/10.1029/2024JD040743, 2024.

Clifton, O. E., Fiore, A. M., Massman, W. J., Baublitz, C. B., Coyle, M., Emberson, L., Fares, S., Farmer, D. K., Gentine, P., Gerosa, G., Guenther, A. B., Helmig, D., Lombardozzi, D. L., Munger, J. W., Patton, E. G., Pusede, S. E., Schwede, D. B., Silva, S. J., Sörgel, M., Steiner, A. L., and Tai, A. P. K.: Dry Deposition of Ozone Over Land: Processes, Measurement, and Modeling, Reviews of Geophysics, 58, e2019RG000670, https://doi.org/10.1029/2019RG000670, 2020.

Coggon, M. M., McDonald, B. C., Vlasenko, A., Veres, P. R., Bernard, F., Koss, A. R., Yuan, B., Gilman, J. B., Peischl, J., Aikin, K. C., DuRant, J., Warneke, C., Li, S.-M., and de Gouw, J. A.: Diurnal Variability and Emission Pattern of Decamethylcyclopentasiloxane (D5) from the Application of Personal Care Products in Two North American Cities, Environmental Science & Technology, 52, 5610-5618, 10.1021/acs.est.8b00506, 2018.

Coggon, M. M., Stockwell, C. E., Xu, L., Peischl, J., Gilman, J. B., Lamplugh, A., Bowman, H. J., Aikin, K., Harkins, C., Zhu, Q., Schwantes, R. H., He, J., Li, M., Seltzer, K., McDonald, B., and Warneke, C.: Contribution of cooking emissions to the urban volatile organic compounds in Las Vegas, NV, Atmos. Chem. Phys., 24, 4289-4304, 10.5194/acp-24-4289-2024, 2024.

Coggon, M. M., Gkatzelis, G. I., McDonald, B. C., Gilman, J. B., Schwantes, R. H., Abuhassan, N., Aikin, K. C., Arend, M. F., Berkoff, T. A., Brown, S. S., Campos, T. L., Dickerson, R. R., Gronoff, G., Hurley, J. F., Isaacman-VanWertz, G., Koss, A. R., Li, M., McKeen, S. A., Moshary, F., Peischl, J., Pospisilova, V., Ren, X., Wilson, A., Wu, Y., Trainer, M., and Warneke, C.: Volatile chemical product emissions enhance ozone and modulate urban chemistry, Proceedings of the National Academy of Sciences, 118, e2026653118, doi:10.1073/pnas.2026653118, 2021.

Dorling, S. R., Davies, T. D., and Pierce, C. E.: Cluster analysis: A technique for estimating the synoptic meteorological controls on air and precipitation chemistry—Method and applications, Atmospheric

Environment. Part A. General Topics, 26, 2575-2581, https://doi.org/10.1016/0960-1686(92)90110-7, 1992.
Duncan, B. N., Yoshida, Y., Olson, J. R., Sillman, S., Martin, R. V., Lamsal, L., Hu, Y., Pickering, K. E., Retscher, C., Allen, D. J., and Crawford, J. H.: Application of OMI observations to a space-based indicator of NOx and VOC controls on surface ozone formation, Atmospheric Environment, 44, 2213-2223, https://doi.org/10.1016/j.atmosenv.2010.03.010, 2010.
Harkins, C., McDonald, B. C., Henze, D. K., and Wiedinmyer, C.: A fuel-based method for updating mobile source emissions during the COVID-19 pandemic, Environmental Research Letters, 16, 065018, 10.1088/1748-9326/ac0660, 2021.
He, J., Harkins, C., O'Dell, K., Li, M., Francoeur, C., Aikin, K. C., Anenberg, S., Baker, B., Brown, S. S., Coggon, M. M., Frost, G. J., Gilman, J. B., Kondragunta, S., Lamplugh, A., Lyu, C., Moon, Z., Pierce, B. R., Schwantes, R. H., Stockwell, C. E., Warneke, C., Yang, K., Nowlan, C. R., González Abad, G., and McDonald, B. C.: COVID-19 perturbation on US air quality and human health impact assessment, PNAS Nexus, 3, 10.1093/pnasnexus/pgad483, 2024.
Hong, Q., Liu, C., Hu, Q., Zhang, Y., Xing, C., Su, W., Ji, X., and Xiao, S.: Evaluating the feasibility of formaldehyde derived from hyperspectral remote sensing as a proxy for volatile organic compounds, Atmospheric Research, 264, 105777, https://doi.org/10.1016/j.atmosres.2021.105777, 2021.
Jacob, D. J.: Introduction to Atmospheric Chemistry, Princeton University Press1999.
Karion, A., Lauvaux, T., Lopez Coto, I., Sweeney, C., Mueller, K., Gourdji, S., Angevine, W., Barkley, Z., Deng, A., Andrews, A., Stein, A., and Whetstone, J.: Intercomparison of atmospheric trace gas dispersion models: Barnett Shale case study, Atmos. Chem. Phys., 19, 2561-2576, 10.5194/acp-19-2561-2019, 2019.
Kim, S.-W., McDonald, B. C., Seo, S., Kim, K.-M., and Trainer, M.: Understanding the Paths of Surface Ozone Abatement in the Los Angeles Basin, Journal of Geophysical Research: Atmospheres, 127, e2021JD035606, https://doi.org/10.1029/2021JD035606, 2022.
Kleinman, L. I.: The dependence of tropospheric ozone production rate on ozone precursors, Atmospheric Environment, 39, 575-586, https://doi.org/10.1016/j.atmosenv.2004.08.047, 2005.
Li, P., Yang, Y., Wang, H., Li, S., Li, K., Wang, P., Li, B., and Liao, H.: Source attribution of near-surface ozone trends in the United States during 1995–2019, Atmos. Chem. Phys., 23, 5403-5417, 10.5194/acp-23-5403-2023, 2023.
McDonald, B. C., Dallmann, T. R., Martin, E. W., and Harley, R. A.: Long-term trends in nitrogen oxide emissions from motor vehicles at national, state, and air basin scales, Journal of Geophysical Research: Atmospheres, 117, https://doi.org/10.1029/2012JD018304, 2012.
McDonald, B. C., McBride, Z. C., Martin, E. W., and Harley, R. A.: High-resolution mapping of motor vehicle carbon dioxide emissions, Journal of Geophysical Research: Atmospheres, 119, 5283-5298, https://doi.org/10.1002/2013JD021219, 2014.
McDonald, B. C., McKeen, S. A., Cui, Y. Y., Ahmadov, R., Kim, S.-W., Frost, G. J., Pollack, I. B., Peischl, J., Ryerson, T. B., Holloway, J. S., Graus, M., Warneke, C., Gilman, J. B., de Gouw, J. A., Kaiser, J., Keutsch, F. N., Hanisco, T. F., Wolfe, G. M., and Trainer, M.: Modeling Ozone in the Eastern U.S. using a Fuel-Based Mobile Source Emissions Inventory, Environmental Science & Technology, 52, 7360-7370, 10.1021/acs.est.8b00778, 2018a.
McDonald, B. C., de Gouw, J. A., Gilman, J. B., Jathar, S. H., Akherati, A., Cappa, C. D., Jimenez, J. L., Lee-Taylor, J., Hayes, P. L., McKeen, S. A., Cui, Y. Y., Kim, S.-W., Gentner, D. R., Isaacman-VanWertz, G., Goldstein, A. H., Harley, R. A., Frost, G. J., Roberts, J. M., Ryerson, T. B., and Trainer, M.: Volatile chemical products emerging as largest petrochemical source of urban organic emissions, Science, 359, 760-764, doi:10.1126/science.aaq0524, 2018b.
Pfannerstill, E. Y., Arata, C., Zhu, Q., Schulze, B. C., Woods, R., Seinfeld, J. H., Bucholtz, A., Cohen, R. C., and Goldstein, A. H.: Volatile organic compound fluxes in the agricultural San Joaquin Valley – spatial distribution, source attribution, and inventory comparison, Atmos. Chem. Phys., 23, 12753-12780, 10.5194/acp-23-12753-2023, 2023.

Rickly, P. S., Coggon, M. M., Aikin, K. C., Alvarez, R. J., II, Baidar, S., Gilman, J. B., Gkatzelis, G. I., Harkins, C., He, J., Lamplugh, A., Langford, A. O., McDonald, B. C., Peischl, J., Robinson, M. A., Rollins, A. W., Schwantes, R. H., Senff, C. J., Warneke, C., and Brown, S. S.: Influence of Wildfire on Urban Ozone: An Observationally Constrained Box Modeling Study at a Site in the Colorado Front Range, Environmental Science & Technology, 57, 1257-1267, 10.1021/acs.est.2c06157, 2023.
Sillman, S.: The use of NO y , H2O2, and HNO3 as indicators for ozone-NO x -hydrocarbon sensitivity in urban locations, Journal of Geophysical Research: Atmospheres, 100, 14175-14188, https://doi.org/10.1029/94JD02953, 1995.
Stohl, A., Forster, C., Frank, A., Seibert, P., and Wotawa, G.: Technical note: The Lagrangian particle dispersion model FLEXPART version 6.2, Atmos. Chem. Phys., 5, 2461-2474, 10.5194/acp-5-2461-2005, 2005.
Verreyken, B., Brioude, J., and Evan, S.: Development of turbulent scheme in the FLEXPART-AROME v1.2.1 Lagrangian particle dispersion model, Geosci. Model Dev., 12, 4245-4259, 10.5194/gmd-12-4245-2019, 2019.
Wang, P., Chen, Y., Hu, J., Zhang, H., and Ying, Q.: Attribution of Tropospheric Ozone to NOx and VOC Emissions: Considering Ozone Formation in the Transition Regime, Environmental Science & Technology, 53, 1404-1412, 10.1021/acs.est.8b05981, 2019.
Wolfe, G. M., Marvin, M. R., Roberts, S. J., Travis, K. R., and Liao, J.: The Framework for 0-D Atmospheric Modeling (F0AM) v3.1, Geosci. Model Dev., 9, 3309-3319, 10.5194/gmd-9-3309-2016, 2016.
Yu, K. A., Li, M., Harkins, C., He, J., Zhu, Q., Verreyken, B., Schwantes, R. H., Cohen, R. C., McDonald, B. C., and Harley, R. A.: Improved Spatial Resolution in Modeling of Nitrogen Oxide Concentrations in the Los Angeles Basin, Environmental Science & Technology, 57, 20689-20698, 10.1021/acs.est.3c06158, 2023.
Zhu, Q., Schwantes, R. H., Coggon, M., Harkins, C., Schnell, J., He, J., Pye, H. O. T., Li, M., Baker, B., Moon, Z., Ahmadov, R., Pfannerstill, E. Y., Place, B., Wooldridge, P., Schulze, B. C., Arata, C., Bucholtz, A., Seinfeld, J. H., Warneke, C., Stockwell, C. E., Xu, L., Zuraski, K., Robinson, M. A., Neuman, J. A., Veres, P. R., Peischl, J., Brown, S. S., Goldstein, A. H., Cohen, R. C., and McDonald, B. C.: A better representation of volatile organic compound chemistry in WRF-Chem and its impact on ozone over Los Angeles, Atmos. Chem. Phys., 24, 5265-5286, 10.5194/acp-24-5265-2024, 2024a.
Zhu, Q., Schwantes, R. H., Stockwell, C. E., Harkins, C., Lyu, C., Coggon, M., Warneke, C., Schnell, J., He, J., Pye, H. O. T., Li, M., Ahmadov, R., Pfannerstill, E. Y., Place, B., Wooldridge, P., Schulze, B. C., Arata, C., Bucholtz, A., Seinfeld, J. H., Xu, L., Zuraski, K., Robinson, M. A., Neuman, J. A., Gilman, J., Lamplugh, A., Veres, P. R., Peischl, J., Rollins, A., Brown, S. S., Goldstein, A. H., Cohen, R. C., and McDonald, B. C.: Co-benefits of the Zero-Emission Vehicle Adoption on CO2 Emissions and O3 Pollution in Los Angeles, in prep., 2024b.